POSTPRINT VERSION. The final version is published here: Gannouni, W., Doumbia, M. L., & Badri, A. (2021). Study on the viability of a microminiature inductive angular position sensor using low-cost fabrication techniques. In Microelectronic Engineering (Vol. 236, pp. 111480). https://doi.org/10.1016/j.mee.2020.111480

Study on the viability of a microminiature inductive angular position sensor using low-cost fabrication techniques

Walid Gannouni[a]*, Mamadou Lamine Doumbia[a], Adel Badri[b]

[a]Electrical and Computer Engineering Department, Université du Québec à Trois-Rivières, C.P. 500, Trois-Rivières, Québec G9A 5H7, Canada
[b]Industrial Engineering Department, Université du Québec à Trois-Rivières, C.P. 500, Trois-Rivières, Québec G9A 5H7, Canada

Abstract

In this study, we propose an inductive angular position sensor comprising thin film, gold spiral inductors on ceramic chips as an alternative to the current state of the art which suffers from limitations in terms of the scope for micro-miniaturization. The geometry of the transmitter and receiver coils, operating frequency, and the air gap between the transmitter and sense coils all influence the performance of the sensor. Herein, we design and fabricate an inductive position sensor based on micro inductors normally employed in the resonant elements of microwave circuits and as chokes in power sources. We use these inductors as both a magnetic field receiver and transmitter and quantify the generated electromagnetic field. This approach has the advantage of providing angular sensing while being substantially easier and more economical to fabricate compared to currently available commercial sensors. The sensor is designed in such a way that the inductance versus angular displacement possesses an arctangent relationship. Due to this feature, the angular position is obtained easily from the sensor signal without the need for complex mathematical calculations, which is not the case for most of the planar coil-based sensors. A prototype of the proposed sensor has been developed and tested. The sensor has an accuracy comparable with much larger existing sensors (residual error standard deviation 2.55% of full scale), a high linearity (R^2 99.3%) and a low sensitivity to injected noise (0.5%). This low-cost, miniature, rotary position sensor could find numerous applications especially in the modern field of automotive engineering.

Keywords: Inductive position sensor, Magnetic field, Micro inductor, Electromagnetic sensing, Eddy current, Angular displacement.

1. Introduction

Inductive sensors are among the most widely used sensors in the automotive industry. However, the large size of these sensors, which is determined by the current manufacturing process, limits their use in modern complex applications. Micromachining processes have been widely used to produce micro touch sensors [1,2] and planar inductor array based angular position sensors [3,4]. The efficacy of various microsensors that use complementary metal-oxide-semiconductor (CMOS) [5] and capacitive [6] detection approaches has been successfully demonstrated. However, special and complex micromachining processes are required to manufacture these sensors. In addition, shrinking the size of electromechanical sensors dramatically decreases their sensitivity and consequently restricts sensor performance [7]. Process consistency and damage to brittle, thin-film structures also become a problem during fabrication and operation.

Recently, there has been more focus on the integration and fabrication of micro-inductors [8,9]. Several design considerations were identified in studies. One study used a triaxial inductive sensor integrated into a CMOS device [1]. Another study employed a three-axis tactile sensor with a four-plane coil and a conducting film implemented with a hyperelastic material [2]. Both these sensors were interfaced using an LDC1614 (Texas Instruments, USA) inductive conversion chip. A further study employed a non-contact motion sensor with two flat coils engraved on a PCB with a ferromagnetic core [3]. This device was interfaced with an LDC1000 converter (Texas Instruments, USA). This sensor has the advantage of producing minimal errors but has a nonlinear input/output relationship. The measurement and calibration methods employed in some studies [10–15] are very complicated and very difficult to apply to the detection of micro displacement on the micrometer scale. One of these recent studies utilized an angular position calibration method with two absolute position sensors yielding an angle error of 4° [14]. These studies also show that as the physical dimensions of the sensor decrease so does the measurement accuracy. We do not consider that such approaches are viable for further reductions in scale.

Our aim in this work is to create the elements of a non-contact, inductive position sensor in micro form that overcomes many of the short comings of the current state of the art as previously identified. In this article, we describe a new generation of micro-inductive sensors that solve the size problem, improve cost effectiveness and ease of fabrication. Specifically, we present a new inductive position sensor based on planar, spiral coils. The sensor is designed in such a way that the relationship between the planar coils and the target provides angular displacement via a non-complex mathematical relationship. Because of this characteristic, positions are easily obtained from the measured signal, which is not the case for most flat-coil sensors which require complex mathematical transformations and consume considerable real-time computing resource. In contrast, with other contactless microelectronic inductive sensor designs [16–19], we do not expect a significant decrease in angular sensing capabilities despite the significant reduction in physical size. A systematic methodology has been adopted to propose a new generation of inductive position sensors. In section 2 the design of a realizable inductive sensor is discussed. Section 3 describes the fabrication of the experimental sensor, using standard, easily available commercial components. Section 4 then proceeds to characterize and quantify the actual performance of the fabricated sensor. The final section summarizes the performance of the experimental sensor and highlights the potential advantages, when compared with other currently available inductive sensors.

2. Material and methods

The proposed planar angular position sensor uses the eddy currents effect principle. The implemented structure, shown in Fig. 1, consists of an excitation coil with two turns (Tx), circular rotatable target made of copper, and two receiver coils (Rx1, Rx2). Each receiver coil comprises two coils connected in series. These discrete thin-film inductors comprise a gold spiral track on a ceramic chip. The purpose of this design is to detect rotation angle, φ, around the Z-axis. The sensor receiver coils Rx1 have clockwise windings placed diametrically opposite to the counterclockwise windings of the receiver coils Rx2. The copper target rotates about the Z-axis above the sensor coils. The sensor parameters are presented in figure 1. The signal injected into the excitation coil generates a time-varying magnetic field, which induces eddy currents in the sensor target, which in turn induces voltages in the sense coils. These voltages are representative of the sensor target angular position. The voltage induced in a sensing coil V_{Rx} is

$$V_{Rx} = M_{TR}\frac{dI_{Tx}}{dt} = M_{TR}\, I_0\, \omega\ \cos(\omega t) \quad (1)$$

where $I_{Tx} = I_0 \, sin\,(\omega t)$, I_0 *is* the peak amplitude of the excitation current, ω is the frequency of excitation, and M_{TR} is the mutual inductance between the excitation and receiver coils.

The voltage induced in the sensing coils V_{Rx1} and V_{Rx2} is now defined with the mutual inductance M_{TR} as a function of the angular position φ of the conductive target. The voltage induced in the sensing coil can now be represented as

$$V_{Rx1} = M_{TR1}\, sin(\varphi) I_0\, \omega \cos(\omega t) = V^0_{Rx1} sin(\varphi) \quad (2)$$

$$V_{Rx2} = M_{TR2}\, cos(\varphi) I_0\, \omega \cos(\omega t) = V^0_{Rx2} \cos(\varphi) \quad (3)$$

The measured angle can be extracted as follows:

$$\frac{V_{Rx1}}{V_{Rx2}} = \frac{V^0_{Rx1} sin(\varphi)}{V^0_{Rx2} cos(\varphi)} = \frac{V^0_{Rx1}}{V^0_{Rx2}} tan(\varphi) \quad (4)$$

$$\varphi = arctan\,(\frac{V_{Rx1}}{V_{Rx2}} k) \quad (5)$$

The normalize the sensor signals, designated as V_{Rx1} and V_{Rx2} are used to obtain target angle via the arctan function in accordance with equation 5.

Element	Parameter	Value	Unit
Excitation coil (Tx)	Outer diameter	5.04	mm
	Inner diameter	4.98	mm
	Gold trace depth	40	µm
	Number of turns	2	
	Excitation frequencies	3.5	MHz
Sensing coils (Rx1, Rx2)	Outer diameter	2	mm
	Gold trace depth	40	µm
	Number of turns	16	
Copper target	Three-quarter circle radius	2.6	mm
	Sensor/target spacing	0.15	mm
	Target thickness	0.3	mm

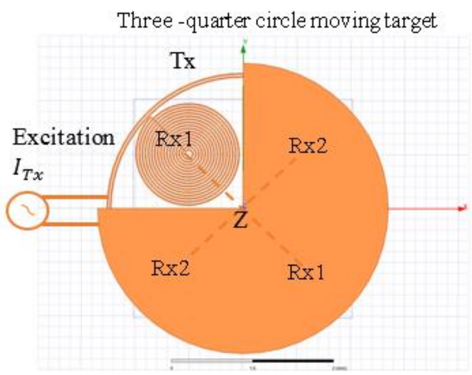

Fig. 1. Proposed sensor design parameters

3. Fabrication and experimental setup

The proposed sensor is fabricated using standard, easily available commercial components commonly used in the manufacture of mobile phones. These components (supplied by Piconics Inc. USA) were assembled manually to produce the complete sensor which is the subject of this paper.

The sensor (Fig. 2) comprises a set of four coils in the middle of a circular transmitter coil. The coils are connected diagonally (with no connection at the center, where the bonding wires cross). The polarity of the sensing coils depends on the current direction in each loop. Each sensing coil has a clockwise winding placed diametrically opposite and connected to a counterclockwise winding. We employed a slow-polymerization epoxy to adjust the placements of the sensing coils within the transmitter coil. The sensor assembly was attached to a glass fiber laminate board adapter (Surface Mount Board Epoxy Glass 37 × 21.5 mm FR4, part number: RE931-05ST, Roth Elektronik).We used a thin wire wedge weld (Hesse & Knipps BondJet 820 configured for a 25-micron aluminum wire) to make the coil connections. A VHX Keyence digital optical microscope and an Olympus SZ61 stereo microscope with a high depth of field and advanced measurement capabilities were used for inspection and photography. A three-quarter circle conductive target in proximity to the sensor substrate is moved in a rotary motion above all the coils.

The testing setup shown in Fig. 3 was used to characterize the rotary contactless inductive position sensor. The sensor was fixed on the positioning stage of the rotation platform. To obtain accurate experimental results, the rotating axes of the rotation stage and the angle sensor are carefully aligned to avoid error due to eccentricity. The positioning test platform incorporates a laboratory calibrated optical angular sensor which delivers a measurement of actual angular position with an accuracy of 15 minutes of arc. The rotation controller and gear controlled the rotation of the copper sensor target. The angular displacement applied to the sensor was controlled by a commercial low-voltage motor controller (RS Components 244-2686 PRO, DC Motor Controller). The unconditioned position signals from the sensor were measured using a commercial oscilloscope (Tektronix, MSO3034 - MSO / MDO). We connected the fabricated micro-inductor receiver coils to an electronic receiver chip ZMID5201 and examined the output using ZMID520x evaluation kit application software to calculate the position. We rotated the target and noted the output amplitudes for each position. The transmitter coil was part of the oscillating circuit, which was stimulated by an onboard high-frequency signal generator.

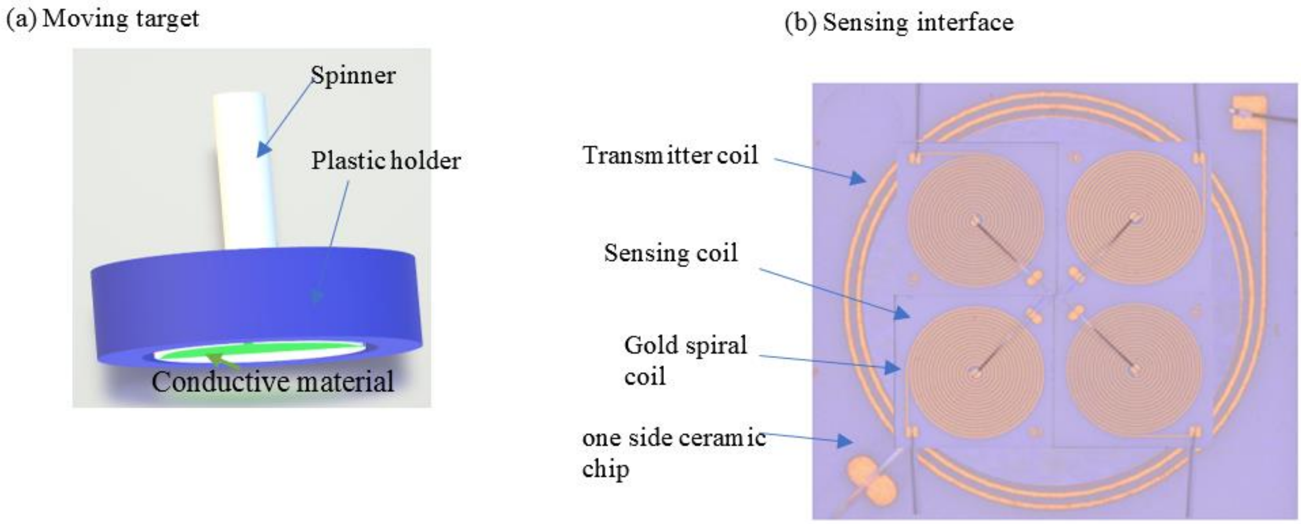

Fig. 2. Fabrication of the angular inductive position sensor comprising a (a) copper sensor target block and (b) gold spiral sensing and excitation coils.

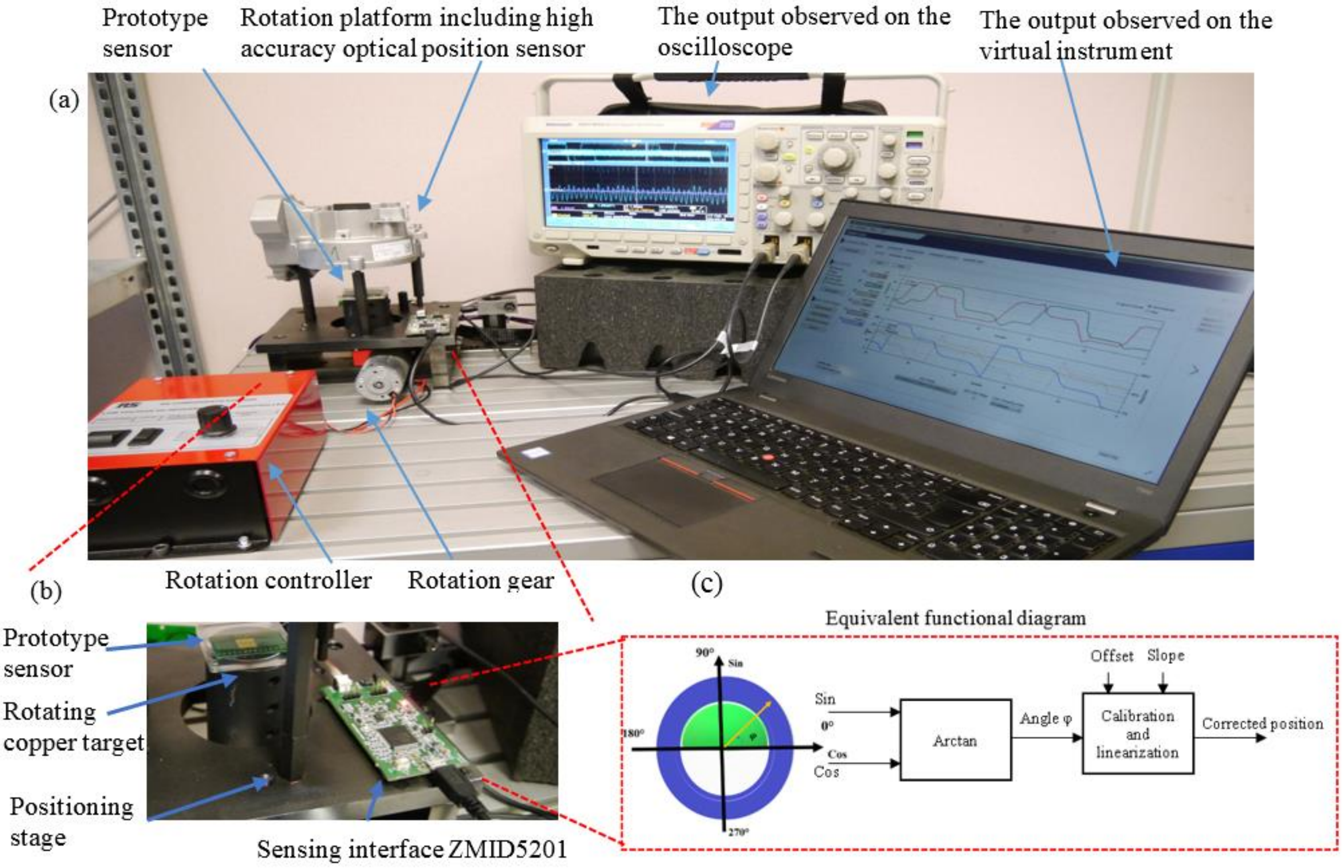

Fig. 3. Measurement setup: (a) experimental setup to measure the variation of the inductive-sensor signal output with a rotation controller, (b) enlarged prototype sensor fixing position, and (c) functional diagram of the sensor-conditioning interface.

The schematic of the inductive sensor interface is summarized in Table 1. The transmit circuitry comprises an LC tank that is formed from the inductance of the transmitting coil and a capacitor on the circuit board. The transmitter coil is connected between EP and EN. The resonant frequency is adjusted with a parallel capacitor CT between EP and EN. The receiver coils are connected across R1 and R2. The pin SOUT is the analog output for an external connection to the computer. The pin VDDE is the external supply voltage with the recommended decoupling capacitor C_{VE}. The bond wire inductance is 2.5 nH with a self-resistance of 0.1 Ω. simplicity, the bond wire inductance and resistance have been incorporated into the respective coil parameters. The sensor generates a magnetic field within the transmitter coil area that is picked up by the receiver coils. The target generates a weak secondary voltage in the sensor coils that varies with rotation angle and can be measured.

Table 1. Specifications and schematic of the of the angular position sensor with detection interfaces of on a commercial integrated circuit ZMID5201

Schematic of the sensor	Electrical specifications of the sensor			
	Element	Parameter	Value	Unit
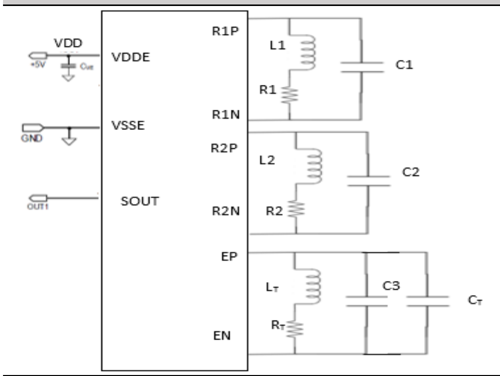	Receiver coil inductance	L1, L2	440.5	nH
	Receiver coil capacitance	C1, C2	0.0064	pF
	Receiver coil resistance	R1, R2	24	Ohms
	Excitation coil inductance	L_T	939.8	nH
	Excitation oscillator capacitor	C_T	2.2	nF
	Excitation coil capacitance	C3	0.0019	pF
	Excitation coil resistance	R_T	6	Ohms
	External supply voltage	VDD	5	V
	Supply capacitor	CVE	100	nF
	Excitation frequency of the transmitter oscillator		3.5	MHz

4. Results and discussion

In this study, we employed the experimental setup shown in Fig. 3 to evaluate the performance of a contactless inductive position sensor with a copper sensor target. Firstly, we rotated the copper sensor block in steps and noted the outputs for each position from the detection interface of Table 1. The target position is indicated by the differential amplitude of the sin and cosine signals measured from the receiver coils. The measured signals, Rx1 and Rx2, in Fig. 4a are converted into an angle in Fig. 4b by implementing the $arctan$ trigonometric function in Eq. 5.

Further, we define calibration parameters for the measured angle. The calibration method provides output calibration with the target in place at operational distance from the receiving coils. The goal of the calibration is to ensure that at opposite ends of the mechanical rotation, the measured positions are zero and the maximum position, respectively. The angle is corrected using the zero offset and gain error to calculate the calibrated position. The measured signals are converted into a measured angle by implementing the arctan trigonometric function. These calculations are implemented using a simple two-dimensional look-up table which is fast and very economical in terms of the required processing resource. A graph showing the corrected position relative to the rotation recorded from the experiment is plotted in Fig. 4b. The results show a linear regression with offset 1.67° and slope 1.0087 (R^2 99.3%) with a residual error standard deviation of 9.2° (2.55% of full scale).

(a) (b)

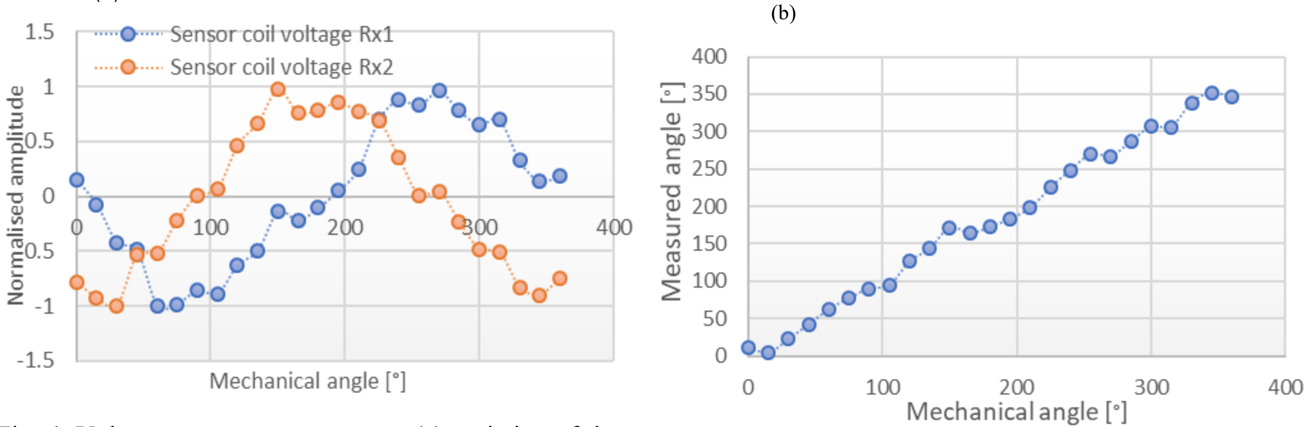

Fig. 4. Voltage output measurements: (a) variation of the signal amplitudes of the sensing coils with rotation angle and (b) output of the measured angle φ as a function of mechanical angle position.

Finally, in this study, we evaluated the performance of the proposed sensor design in the presence of white noise from a noise generator magnetically coupled to the sensor. The rms magnetic noise field at the plane of the sensor was calculated to be 0.26 Gauss. Measurements were performed to identify the influence of this noise on the operation of the sensor. The results shown in Fig. 5 represent the output of the sensor obtained using the same methodology as in Fig. 4. The results again show a linear regression with offset 3.7° and slope 1.027 (R^2 98.8% giving a noise sensitivity 0.5%). The residual error standard deviation is increased by 2.9° to 12.1° (3.36% of full scale).

Inductive sensors usually suffer from noise owing to proximity with interfering electromagnetic fields and environmental contaminants. This may be avoided through the incorporation of appropriate electromagnetic and mechanical shielding.

(a) (b)

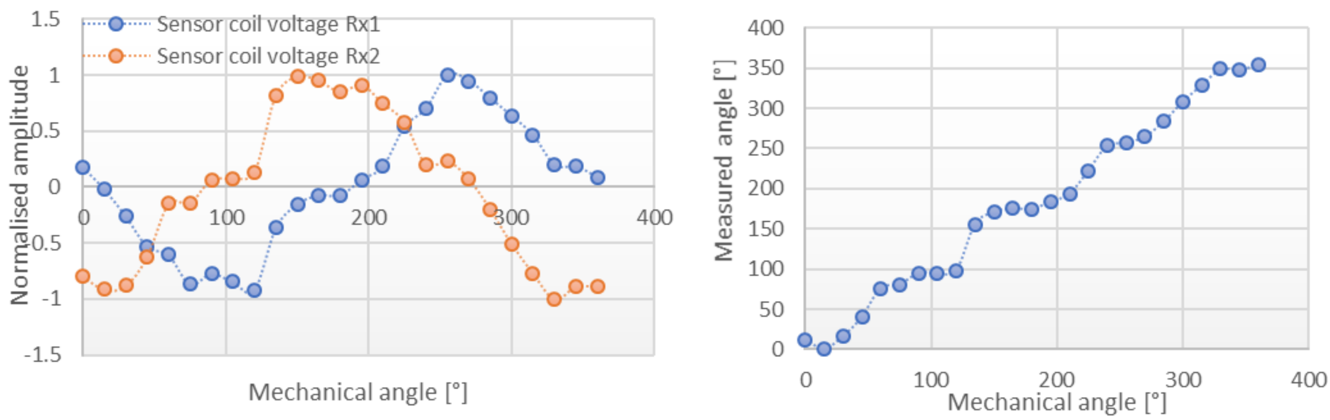

Fig. 5. Voltage output measurements in the presence of white noise: (a) variation of the signal amplitudes of the sensing coils with rotation angle and (b) output of the measured angle φ as a function of mechanical angle.

The proposed planar angular position sensor functions in the same manner as the sensor proposed in a previous study [20].

The fundamental difference is one of scale. The proposed sensor is reduced in size by almost a factor of 10 (5 mm as opposed to 45 mm). The actual accuracy was measured to be of the order of 9.2°. There is scope for further work to improve the accuracy of the proposed sensor.

The sensor prototype was assembled manually using standard, easily available commercial components commonly used in the manufacture of mobile phones. The cost of each spiral chip inductor is less than 20 cents and the interface circuit (ZMID5201) is less than 2.76 dollars. The total cost of the sensor is less than 3.76 dollars. There is potentially a decrease in angular sensing capabilities due to the significant reduction in physical size. However, the sensor has an accuracy comparable with much larger existing sensors. One example with an approximate size of 60 mm claims to achieve accuracies approaching 4° [14] in contrast to the proposed sensor which exhibits an accuracy of 9.2° but has a size of 5 mm. A commercially available miniature angle sensor costing 135 dollars (Novotechnik RFC-4853-636-121-501) has a measurement accuracy of 10° and a physical size of 48 mm.

Inductive position sensors are among the most widely used sensors in automotive applications to measure high-speed mechanical position. This low-cost, miniature, rotary position sensor is ideally suited to these automotive applications, for example, valve and pedal position sensing, where the immunity to electrical noise is a great advantage.

5. Conclusion

A novel concept of angular inductive measurement using thin-film spiral inductors deposited on ceramic chips on the millimeter scale was designed and found to perform satisfactorily. It is substantially easier and less costly to fabricate than some other comparable sensors using different techniques. The designed planar inductor was analyzed using an integrated circuit, and its measurements were compared with other commercially available sensors. The accuracy was measured to be of the order of 9.2°. The accuracy was found to degrade in the presence of electromagnetic noise to approximately 12.1°, but it is anticipated that this could be avoided through appropriate incorporation of shielding into the sensor packaging. This study has demonstrated the viability of the proposed approach to produce extremely small and cost-effective inductive angular position sensors. Moreover, there is scope for further work to improve the accuracy and durability of the proposed sensor.

Declaration of Competing Interest

The authors declare that there are no competing interests.

Acknowledgements

This work was supported by the Canadian National Research Organization Mitacs [grant number IT11495]. The authors would like to thank Simon Pyatt, Senior Research Technician at the Birmingham Instrumentation Laboratory for Particle Physics and Applications (BILPA) of Birmingham University, United Kingdom for his kind assistance and Piconics Inc. for the provision of thin film micro-inductors.

Highlights:

- A new inductive position sensor based on spiral coils with microelectronic technology is presented in this research.
- We explore the possibility of significant miniaturization of angular position inductive sensors.
- Angular sensing substantially easier and less costly fabrication compared with other alternative technologies.
- The sensor has a residual error standard deviation of 2.55% of full scale, a high linearity with R^2 of 99.3% and a very low sensitivity to injected noise of 0.5%.

References

[1] S. Yeh and W. Fang, "Inductive Micro Tri-Axial Tactile Sensor Using a CMOS Chip With a Coil Array," in IEEE Electron Device Letters, vol. 40, no. 4, pp. 620–623, April 2019. DOI: 10.1109/LED.2019.2901946.

[2] H. Wang, D. Jones, G. de Boer, J. Kow, L. Beccai, and A. Alazmani, "Design and Characterization of Tri-Axis Soft Inductive Tactile Sensors," in IEEE Sensors Journal, vol. 18, no. 19, pp. 7793–7801, 1 Oct.1, 2018. DOI: 10.1109/JSEN.2018.2845131.

[3] K. R. Sandra, A. S. A. Kumar, B. George and V. J. Kumar, "A Linear Differential Inductive Displacement Sensor With Dual Planar Coils," in IEEE Sensors Journal, vol. 19, no. 2, pp. 457–464, 15 Jan.15, 2019. DOI: 10.1109/JSEN.2018.2877209.

[4] P. Sagar, H.K. Hassan, A.S. Gour, and R. Karunanithi, "Multilayer planar inductor array based angular position sensor for cryogenic application," Elsevier Cryogenics Journal, Vol. 96, pp. 18–24, 2018, ISSN 0011-2275. https://doi.org/10.1016/j.cryogenics.2018.10.001.

[5] C.-L. Lu and M.-K. Yeh, "Thermal stress analysis for a CMOS-MEMS microphone with various metallization and materials," Elsevier Microelectronic Engineering Journal, vol. 213, pp. 47–54, 15 May 2019. https://doi.org/10.1016/j.mee.2019.04.013.

[6] Y. Hata, Y. Suzuki, M. Muroyama, T. Nakayama, Y. Nonomura, R. Chand, H. Hirano, Y. Omura, M. Fujiyoshi, and S. Tanaka, "Integrated 3-axis tactile sensor using quad-seesaw-electrode structure on platform LSI with through silicon vias," Sensors and Actuators A: Physical, vol. 273, pp. 30–41, Apr. 2018. https://doi.org/10.1016/j.sna.2018.02.013.

[7] K. V. Poletkin, A. I. Chernomorsky, and C. Shearwood, “Proposal for micromachined accelerometer, based on a contactless suspension with zero spring constant,” in IEEE Sensors Journal, vol. 12, no. 7, pp. 2407–2413, July 2012. DOI: 10.1109/JSEN.2012.2188831.
[8] M.L.F. Bellaredj, C.A. Pardue, P. Kohl, and M. Swaminathan, “Fabrication of package embedded spiral inductors with two magnetic layers for flexible SIP point of load converters in Internet of Everything devices,” Elsevier Microelectronic Engineering Journal, vol. 189, pp. 18–27, 5 April 2018. https://doi.org/10.1016/j.mee.2017.12.012.
[9] B. Bardet, S. Desplobain, J. Billoué, L. Ventura, and G. Gautier, “Integration of low-loss inductors on thin porous silicon membranes,” Elsevier Microelectronic Engineering Journal, vol. 194, pp. 96–99, 5 July 2018. https://doi.org/10.1016/j.mee.2018.03.020.
[10] N. Anandan and B. George, “Design and development of a planar linear variable differential transformer for displacement sensing,” IEEE Sensors Journal, vol. 17, no. 16, pp. 5298–5305, Aug. 2017. DOI: 10.1109/JSEN.2017.2719101.
[11] R. Zhang, H. Liu, Y. Zhou, Z. Yang and J. Han, "Design and Analysis of a Mutual Inductance Coupling-Based Microdeformation Sensor," in IEEE Transactions on Instrumentation and Measurement, vol. 66, no. 4, pp. 821-829, April 2017.
[12] S. Kim et al., "An Inductive 2-D Position Detection IC with 99.8% Accuracy for Automotive EMR Gear Control System," in IEEE Transactions on Very Large Scale Integration (VLSI) Systems, vol. 25, no. 5, pp. 1731-1741, May 2017.
[13] Gao, Z.; Zhou, B.; Hou, B.; Li, C.; Wei, Q.; Zhang, R. Self-Calibration of Nonlinear Signal Model for Angular Position Sensors by Model-Based Automatic Search Algorithm. Sensors 2019, 19, 2760.
[14] Jong-Ahn Kim, Jae Wan Kim, Chu-Shik Kang, Jae Yong Lee, Jonghan Jin, On-machine calibration of angular position and runout of a precision rotation stage using two absolute position sensors, Measurement, Volume 153, 2020, 107399, ISSN 0263-2241, https://doi.org/10.1016/j.measurement.2019.107399.
[15] Hongye Liu, Hao Wang, Yan Lyu, Cunfu He, Zenghua Liu, A novel triboelectric nanogenerator based on carbon fiber reinforced composite lamina and as a self-powered displacement sensor, Microelectronic Engineering, Volume 224, 2020, 111231, ISSN 0167-9317, https://doi.org/10.1016/j.mee.2020.111231.
[16] V.F.G. Tseng and H. Xie, “Resonant Inductive Coupling-Based Piston Position Sensing Mechanism for Large Vertical Displacement Micromirrors,” Journal of Microelectromechanical Systems, vol. 25, no. 1, pp. 207–216, Feb. 2016. DOI: 10.1109/JMEMS.2015.2499301.
[17] S.M. Djuric, “Performance analysis of a planar displacement sensor with inductive spiral coils,” IEEE Transactions on Magnetics, vol. 50, no. 4, pp. 1–4, Apr. 2014. DOI: 10.1109/TMAG.2013.2288273.
[18] A. S. Anil Kumar and B. George, "A Noncontact Angle Sensor Based on Eddy Current Technique," in IEEE Transactions on Instrumentation and Measurement, vol. 69, no. 4, pp. 1275-1283, April 2020, doi: 10.1109/TIM.2019.2908508.
[19] S.-K. Yeh, J.-H. Lee, and W. Fang, “On the detection interfaces for inductive type tactile sensors,” Sensors and Actuators A: Physical, Vol. 297, 111545, 2019, ISSN 0924-4247. https://doi.org/10.1016/j.sna.2019.111545.
[20] B. P. Reddy, A. Murali and G. Shaga, "Low cost planar coil structure for inductive sensors to measure absolute angular position," 2017 2nd International Conference on Frontiers of Sensors Technologies (ICFST), Shenzhen, 2017, pp. 14-18, doi: 10.1109/ICFST.2017.8210463.